Journal of
Mechanical
Science and
Technology

Journal of Mechanical Science and Technology 21 (2007) 486~494

Heat/Mass Transfer Characteristics in the Near-Tip Region on a Turbine Blade Surface Under Combustor-Level High Inlet Turbulence

Hyun Goo Kwon[a], Sang Woo Lee[a,*]

[a]*School of Mechanical Engineering Kumoh National Institute of Technology Gumi, Gyeongbuk 730-701, Korea*

(Manuscript Received March 2, 2006; Revised June 27, 2006; Accepted January 19, 2007)

Abstract

Heat/mass transfer characteristics on the near-tip blade surface under combustor-level high inlet turbulence have been investigated within a high-turning turbine rotor passage by using the naphthalene sublimation technique. The inlet turbulence intensity and length scale are 14.7% and 80 mm, respectively. The tip gap-to-chord ratio is changed to be *h/c* = 0.74, 1.47, and 2.94 percents. Increasing *h/c* results not only in higher heat/mass transfer in the pressure-side tip region but also in more convective transport on the pressure surface even far away from the tip edge. Severe heat/mass transfer is always observed in the suction-side tip-leakage flow region which can be divided into two distinct high transport regions. There is a local maximum of heat/mass transfer along the trailing-edge centerline. This arises from the interaction of a tip-leakage vortex with a trailing-edge vortex shedding. Comparisons of the present data for *h/c* = 2.94 percents with the previous low turbulence one show that there is a large discrepancy of heat/mass transfer in the pressure-side near-tip area, which diminishes with departing from the tip edge. The suction-side heat/mass transfer in the tip-leakage flow region is less influenced by the high inlet turbulence than that at the mid-span. The leading-edge heat/mass transfer under the high inlet turbulence is always higher than that in the low turbulence case, while there is no big difference in the trailing-edge heat/mass transfer between the two cases.

Keywords: Gas turbine, Turbine rotor blade, Heat transfer, Tip clearance gap, High inlet turbulence

1. Introduction

The clearance gap between the tip of a turbine rotor blade and the adjacent stationary casing wall forms a narrow flow passage. Due to the presence of pressure difference between the pressure and suction sides of the blade, there exists a strong leakage flow through the tip gap. This undesirable leakage flow delivers not only an aerodynamic loss penalty but also an additional thermal loading to the blade tip. The tip region is exposed to hot gases on all sides and difficult to cool, which could lead to tip burnout. Thus it is very important to understand detailed heat transfer characteristics in the near-tip area for efficient tip cooling schemes.

Early studies on the turbine blade tip heat transfer were conducted on idealized tip models, not in a cascade. Chyu et al. (1989) investigated heat transfer with turbulent flow over shrouded rectangular cavities simulating the tip region of a grooved rotor blade. Metzger and Rued (1989), and Rued and Metzger (1989) studied the influence of turbine tip gap leakage on the flow and heat transfer for a simulated simple geometry on the pressure and suction sides, respectively. They concluded that flow leakage from the turbine tip gap into the suction side results in more extensive and complex heat transfer effects than those for the pressure side. Metzger et al. (1991) used a numerical computation of leakage flow to link a

*Corresponding author. Tel.: +82 54 478 7296; Fax.: +82 54 478 7319
E-mail address: swlee@kumoh.ac.kr

simple flow and heat transfer model to specific turbine geometry and operating point for which a unique set of measured local tip and shroud heat fluxes are available. Jin and Goldstein (2003) carried out local mass transfer measurements on a turbine blade surface for tip gap-to-chord ratios of h/c = 0.86, 1.72, 3.45, and 6.90 percents mainly at a low turbulence level of 0.2 percents. This work seems to be the only heat transfer measurements on a real near-tip blade surface, despite many studies on the tip surface (Bunker et al., 2000; Azad et al., 2000; Papa et al., 2003). Lee and Kwon (2004) investigated heat/mass transfer in the tip-leakage flow region of a high-turning turbine rotor blade for h/c = 2.94 at Tu = 0.3 percents, and compared their data with those in the three-dimensional flow region near the turbine endwall.

Turbine blades are usually exposed to combustor-level high inlet turbulence. However, there seems to be no previous study which deals with the near-tip thermal load on the turbine blade surface under the high inlet turbulence. In this study, the near-tip blade surface heat/mass transfer under the combustor-level high inlet turbulence has been investigated within a high-turning turbine rotor passage for three different h/c's. One of these results is compared with the previous low turbulence data.

2. Experiment

2.1 Linear turbine cascade with tip gap

The cascade wind tunnel comprises an open-circuit type wind tunnel, a high turbulence generator, an inlet duct, and a linear turbine cascade with tip clearance gap, and an exhaust section. The wind tunnel has a cross section of 0.6 m×0.4 m, and the inlet duct has a cross section of 0.42 m×0.32 m. The flow coming out from the high turbulence generator is developing to a turbulent boundary-layer flow on the top and bottom walls of the inlet duct, after passing a trip wire of 1.8 mm in diameter and sand paper. As shown in Fig. 1, the turbine cascade has six linear turbine blades, and its entrance is located 1.20 m downstream of the exit of the turbulence generator. The high turbulence generator employed in this study is designed to simulate the highly turbulent flow from a combustor. Its details were reported by Lee et al. (2004).

The blades are fabricated in a large scale based on

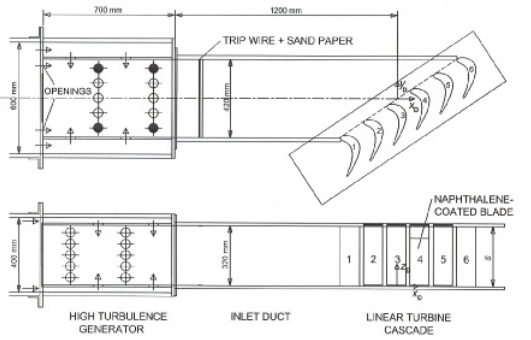

Fig. 1. Overall view of cascade wind tunnel with tip clearance gap.

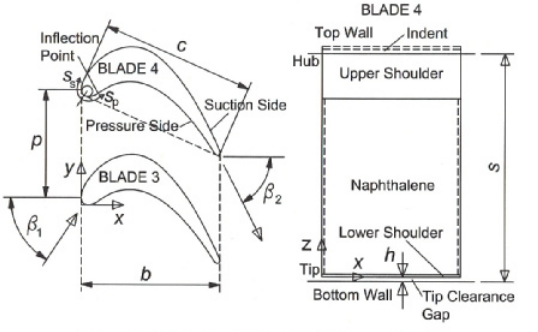

Number of blades	6
Chord length (c)	217.8 mm
Axial chord (b)	196.0 mm
Pitch (p)	151.6 mm
Span (s)	320.0 mm
Blade inlet angle (β_1)	56.4 deg
Blade outlet angle (β_2)	-62.6 deg

Fig. 2. Arrangement of turbine blade cascade.

the mid-span profile of a first-stage turbine rotor blade, and they are made of an engineering plastic (Ivory MC Nylon). As can be seen in Fig. 1, the four blades in the middle have a tip gap, but the two far-end blades of #1 and #6 act as guide vanes with no tip gap. As shown in Fig. 2, the tip gap near the bottom wall can be achieved by inserting each upper end of the blade into the indent situated on the top wall. As listed in Fig. 2, the chord, c, axial chord, b, pitch, p, and span, s, are 217.8 mm, 196.0 mm, 151.6 mm, and 320.0 mm, respectively. The span in this study is determined, based on the aspect ratio of the original blade of s/c = 1.47. The turning angle of this rotor blade is given as 119.0 degrees. The rotor blade profile used in this study is reported by Jun (2000).

The coordinates of the inlet duct, $x_D y_D z_D$, has their origin on the bottom wall at the center of the central blade passage in the inlet plane of the cascade (Fig. 1). In the *xyz* coordinates (Fig. 2), *x*, *y*, and *z* are in the axial, pitch-wise and span-wise directions of the cascade. The *z*-directional coordinate starts from the tip edge. In addition to these rectangular ones, two curvilinear coordinates, s_p and s_s, are defined as in Fig. 2 along the blade pressure and suction surfaces, starting at an intersection of the blade profile with a line drawn upstream from the center of the leading edge circle at the blade inlet angle.

2.2 Naphthalene sublimation technique

In this technique, mass transfer coefficient, h_m, is evaluated from the corresponding sublimation depth of cast naphthalene. The local Sherwood number, Sh, which is commonly used as a dimensionless mass transfer coefficient, is defined as

$$\mathrm{Sh} = (h_m c)/D \tag{1}$$

where *D* is the diffusion coefficient of naphthalene in air. According to an analogy between heat and mass transfer (Goldstein and Cho, 1995), the Nusselt number can be obtained in the following way.

$$\frac{\mathrm{Nu}}{\mathrm{Sh}} = \left(\frac{\mathrm{Pr}}{\mathrm{Sc}}\right)^n \tag{2}$$

where *n* is usually taken to be 1/3 for a laminar flow and to be 0.4 for a turbulent one. The boundary condition in the mass transfer system is equivalent to the constant surface temperature condition in the heat transfer system.

2.3 Naphthalene coated blade and profile measuring system

The test blade to be coated with naphthalene is presented on the right side in Fig. 2 and is made of aluminum. Its molds are the same as those used by Lee et al. (2005). The cast blade has upper and lower metal shoulders of 70 and 2.4 mm in width respectively. A thin layer of naphthalene of 2 mm in thickness is cast on the recess of the cast blade between the two metal shoulders. Its length is 250 mm. This cast test blade is positioned at the location of the blade #4 as in Fig. 1. Its upper metal shoulder is inserted into an indent machined on the top wall of the cascade. A T-type thermocouple is embedded in the cast naphthalene to obtain the naphthalene surface temperature during the sublimation experiments.

In order to measure sublimation depth on a curved surface such as a turbine blade, which has a local curvature varying around its surface, a depth gauge should be oriented normal to the surface. We use the same device that was used by Lee et al. (2005). As shown in Fig. 3, this profile measuring system has not only a three-dimensional traversing mechanism for the depth-gauge movement but also a blade rotator installed on a robust frame structure. Sublimed depth is measured at 62 points around the blade and at 15 points in the *z*-direction. The measurement locations are populated densely near the tip as well as on the leading- and trailing-edges. The measurement locations in the *z*-direction range from 4.0 to 160 mm from the lower end of the test blade. During the scanning of the whole measurement locations, three sequential procedures of a rotation of the cast blade at a proper angle, a following three-dimensional adjustment of the depth gauge, and scans of it in the span-wise direction are repeated.

2.4 Data reduction systems

The measurements of velocity, turbulence, temperature and naphthalene sublimation depth are controlled by a personal computer (IBM, AT 486) equipped with plug-in boards such as a Multi-Function DI/O Board (National Instruments, AT-MIO-16D-H-9) and a GPIB adapter (National Instruments, AT-GPIB). Velocities are measured with a digital micromonometer (Furness Controls, FCO12). Temperatures

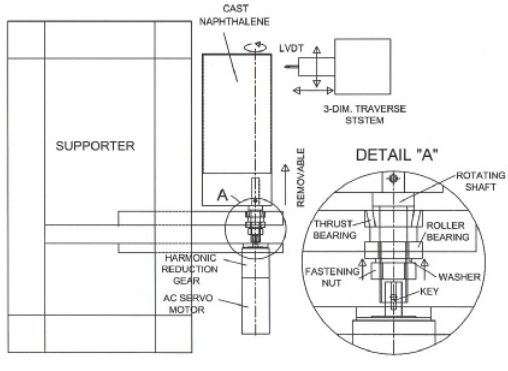

Fig. 3. Schematic diagram of four-axis profile measuring system.

of the free-stream and cast naphthalene are measured with T-type thermocouples connected to a digital voltmeter (Keithley, Model 2001TSCAN), which is controlled by the computer through the GPIB. Thermocouples are calibrated using a constant-temperature bath (Fisher Scientific, 9010) and a standard thermometer. The temperature measurements are based on the STP 470A (1974) published by ASTM. In the measurements of turbulence intensity and integral length scale, a hot-wire anemometer (Kanomax, model 1010) is used.

A LVDT (linear variable differential transformer) depth gauge (Sensortec, 060-3590-02) is used to measure the local sublimation depth. Its full scale and resolution are ±1.0 mm and 1.0 μm, respectively. When a smooth solid surface of naphthalene is obtained from the cast procedure, the test blade is mounted on the rotating shaft as in Fig. 3. Then, the first scanning of the naphthalene surface is conducted with the calibrated depth gauge at 930 locations, before exposure to the air flow. It takes about 50 minutes to complete the total scanning. The readings of local elevation are recorded in the computer through the 12-bit A-D converter. Then, the cast blade is positioned in the cascade. After it is exposed to the air flow for about 90 minutes, it is brought back to the profile measuring system, and is scanned again. The difference between the before-and-after readings at each location still includes free-convection loss during the setup time of the cast blade as well as during the depth measurements. This extra sublimation depth is typically about 7.5 percent of the average sublimation depth. The net sublimation depth is finally obtained after a proper correction.

2.5 Operating conditions and uncertainties

During the sublimation experiments, the free-stream velocity in the inlet duct at x_D/c = -1.5 is maintained at U_∞ = 15 m/s. A good pitch-wise mean flow periodicity is obtained at the entrance of the central three blade passages within 2 percent deviation. The inlet Reynolds numbers based on the free-stream velocity and the chord, Re_∞, is 2.09×10^5. The inlet turbulence intensity and integral length scale measured at x_D/c = -1.5 are 14.7 percents and 80 mm, respectively. The boundary-layer thickness, displacement thickness, and momentum thickness measured on the bottom wall at x_D/c = -0.23 are 28.0 mm, 2.28 mm, and 1.92 mm, respectively. In this study, the tip gap with respect to the chord is changed to be h/c = 0.74, 1.47, and 2.94 percents. During exposure of the cast blade to the cascade air flow, naphthalene surface temperature is kept within 0.2 °C. The uncertainty interval of Sh with 95 percent confidence based on Abernethy et al. (1985) is estimated to be ±7.6 percents of Sh.

3. Results and discussion

3.1 Contours of Sh on the pressure surface

Contours of Sh on the pressure surface for h/c = 0.74, 1.47, and 2.94 percents are shown in Fig. 4. Based on the Sh distributions, the entire pressure surface can be classified into several regions such as the leading-edge region, the trailing-edge region, the near-tip region, and the other, regardless of h/c. The value of Sh is very high at the leading-edge region and suffers a steep decrease to a value lower than 600 in the range between s_p/c = 0.07 and 0.13, where there occurs a laminar flow separation around the inflection point. After this, Sh increases rapidly due to the reattachment of the separated flow. Then, it decreases mildly until the trailing edge is reached. Again, there is higher mass transfer on the trailing edge. The region between the mid-chord and the trailing edge, the variation of Sh is found to be very small.

These mid-span trends are not true for the mass transfer near the blade tip. Due to the pressure difference between the pressure and suction sides, there is a strong leakage flow toward the suction side through the tip gap. Before entering the tip gap, the flow tends to be accelerated over the pressure-side tip edge, which leads to mass transfer augmentation in the near-tip region. This is why the contours near the tip edge at z/s = 0.0 become horizontal as in Fig. 4. With increasing h/c, Sh in the pressure-side tip region tends to increase, because wider gap results in stronger tip-leakage flow. This stronger leakage flow at higher h/c adds more z-directional (span-wise) velocity component to the velocity field, which results in more convective transport on the pressure surface even far away from the tip edge. Therefore, Sh on the pressure surface even away from the tip edge become higher as h/s increases. As can be seen in Fig. 4, it is clear that with the increment of h/c, Sh on the leading edge increases and the area surrounded by the contour of Sh = 600 at around s_p/c = 0.1 becomes narrower.

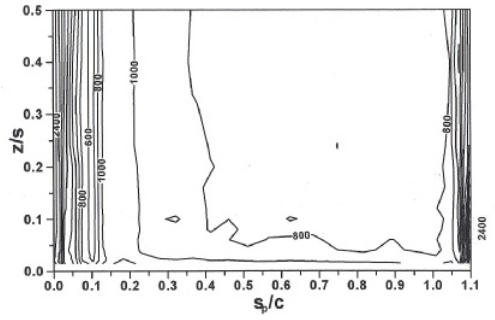

(a) h/c = 0.74%

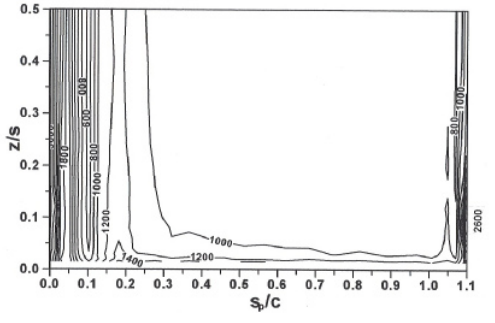

(b) h/c = 1.47%

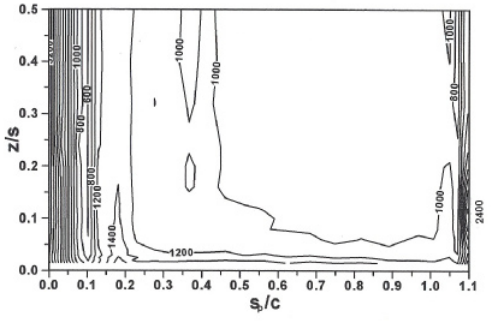

(c) h/c = 2.94%

Fig. 4. Contours of Sh on the pressure surface.

It is very interesting that there is a local peak of Sh away from the tip edge along the trailing-edge centerline of about s_p/c = 1.1. This local maximum at the trailing edge is found for all three h/c's and its position become farther away from the tip edge as h/s increases. Previous study with no tip gap (Lee et al., 2005) showed that the local maximum along the trailing-edge centerline is located at z/s = 0. A close examination shows that the maximum of Sh all over the pressure surface is found at around s_p/c = 1.1 for h/c = 0.74 percents but at around s_p/c = 0 for h/c = 1.47 and 2.94 percents. In other word, the highest thermal load is observed at the trailing edge for the lowest tip gap but at the leading edge for the higher tip gaps. Therefore, a special care should be taken in the trailing-edge cooling scheme. These local peaks of Sh at the trailing edge are resulted from the interaction of a tip-leakage vortex developing along the suction side with a vortex shedding behind the trailing edge, so that the span-wise location of the local peak coincides approximately with the elevation of the tip-leakage vortex center.

3.2 Contours of Sh on the suction surface

Contours of Sh on the suction surface for h/c = 0.74, 1.47, and 2.94 percents are shown in Fig. 5. The local Sh distribution on the suction surface is different totally from that on the pressure side in Fig. 4. As on the pressure side, the entire suction surface can be classified into the leading-edge region, the trailing-edge region, the near-tip region, and the other. In the leading-edge region, there is very high Sh and its value increases with the increment of h/s. In the trailing-edge region, a high gradient of Sh is found due to the rapid flow change in a narrow area. In the near-tip region, there is a broad area of very high Sh along the tip edge as well. Strictly speaking, this near-tip region with high mass transfer is divided into two regions: the upstream high transport region and the downstream high transport region. In Fig. 5(b), for example, the former has a narrow area very close to the tip edge at between about s_s/c = 0.15 and 0.4, but the latter has a much wider area from the tip edge to z/s = 0.2 at between about s_s/c = 0.6 and 1.4. With increasing h/s from 0.74 to 2.94, the maximum value of Sh in the upstream high transport region increases from about 1400 to 2200, but that in the downstream high transport region decreases from about 2800 to 2200. Therefore, the maximum values of Sh in the upstream and downstream regions have nearly the same value of about 2200 when h/s = 2.94. With increasing h/s, the upstream high transport region becomes longer in its shape and the local peak of Sh in the downstream high transport region moves farther away from the tip edge with decreasing Sh gradient.

On the assumption that tip-leakage flow makes local mass transfer augmented, the Sh distributions near the tip in Fig. 5 suggest that there are two channels through which the leakage flow comes out of the tip gap. The upstream and downstream high transport regions mentioned earlier could be considered

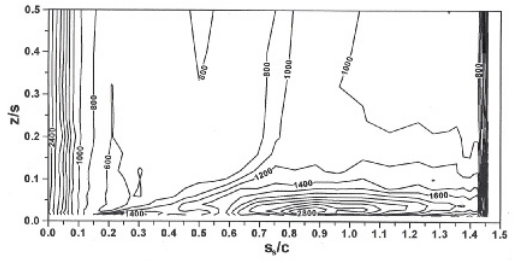

(a) h/c = 0.74%

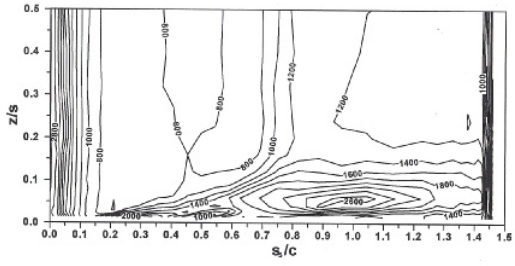

(b) h/c = 1.47%

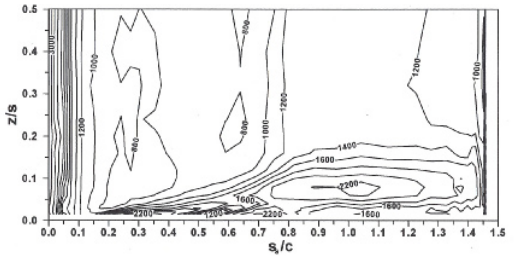

(c) h/c = 2.94%

Fig. 5. Contours of Sh on the suction surface.

sidered as the exits of the channel. There seems to be a small amount of the leakage flow through the former because mass transfer enhancement is occurred in a confined narrow area. On the other hand, most of the leakage flow seems to come out of the tip gap through the latter. Bindon (1989) assumed that there are two channels of the leakage flow, a tiny upstream one and a major mid-chord one in Fig. 8 of his study. The tiny upstream channel is located just downstream of the leading edge, and the flow through it is named as a "separated vortex". Most of the leakage flow, however, passes the major mid-chord channel. Present mass-transfer data could verify the suggestion by Bindon (1989) and identify the locations of his two channels.

3.3 Distributions of Sh in a low turbulence case

In order to understand the effects of the combustor-level high inlet turbulence on the blade-surface heat/mass transfer in the near-tip region, the present result is compared with an available low-turbulence one for h/c = 2.94 percents by Lee and Kwon (2004). Their inlet turbulence intensity has a very low level of 0.3 percents, but the blade geometry and Reynolds number are all the same for the two cases.

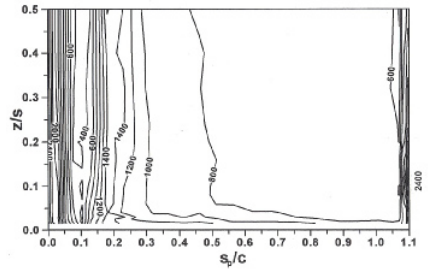

(a) Pressure surface

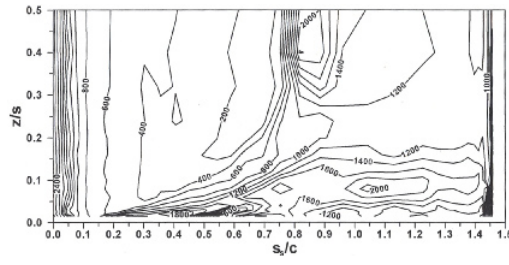

(b) Suction surface

Fig. 6. Contours of Sh in the low turbulence case for h/c = 2.94%.

Contours of Sh on the pressure surface in the low turbulence case are shown in Fig. 6(a). The comparison of Sh between the low and high turbulence cases (Fig. 6(a) and Fig. 4(c)) shows that the present high turbulence level (Tu = 14.7 percents), in general, provides a more uniform distribution of Sh. Near the tip edge (z/s = 0.0), there are higher mass transfer and wider tip-leakage area in the high turbulence case. In both the low and high turbulence cases, there is a local peak of Sh along the trailing-edge centerline away from the tip edge. Independent of the inlet turbulence, this peak value are nearly the same as high as about 2400 at the same span-wise elevation, which implies that the interaction of the tip-leakage vortex with the trailing-edge vortex shedding is not much influenced by the inlet turbulence.

The suction-side Sh distribution in the low turbulence case (Fig. 6(b)) in general shows the same qualitative trend as that in the high turbulence case (Fig. 5(c)), particularly in the leading- and trailing-

edge regions and in the near-tip region. At the mid-span, however, the steep gradient of Sh at between s_s/c = 0.7 and 1.0 found in Fig. 6(b) is not existent in the high turbulence case any more. The near-tip region can be divided into the upstream high transport region and the downstream one, regardless of the inlet turbulence level. Judging from Fig. 5(c) and Fig. 6(b), the near-tip mass transfer is less influenced by the high inlet turbulence than the mid-span one. This is because local high turbulence is already produced in the leakage flow region due to the strong interaction between the leakage jet from the tip gap and the cascade passage flow.

3.4 Direct comparisons of Sh between the low and high turbulence cases

Figure 7 shows the direct comparisons between the low and high turbulence cases at different span-wise locations. The comparisons provide that the high inlet turbulence generally results in higher Sh regardless of *z/s*. At the leading edge, there always exists a high spike of Sh even near the tip edge such as *z/s* = 0.02. Its value in the high turbulence case is always higher than that in the low turbulence case. On the pressure surface, Sh in the high turbulence case is not only higher but also more uniform than that in the low turbulence case, regardless of *z/s*. There is a big difference in the pressure-side value of Sh between the two cases, particularly between the mid-chord and trailing edge at *z/s* = 0.02, but this difference diminishes with increasing *z/s*. The comparisons also show that the abrupt variation of Sh near the inflection point (s_p/c = 0.1) on the pressure side is less severe in the high turbulence case. On the suction surface, Sh at *z/s* = 0.02 suffers a dramatic variation in the range of $0.1 < s_s/c < 0.8$. Regardless of the inlet turbulence, there are two local minimums and two local maximums in this region, which demonstrates the existence of the tiny upstream channel of the tip-leakage flow assumed by Bindon (1989). Even very close to the tip edge as in Fig. 7(a), the high inlet turbulence not only delivers higher Sh but also reduces local variation of Sh on the suction surface. At *z/s* = 0.12, Sh on the suction surface has a totally different tendency from that at *z/s* = 0.02. The high inlet turbulence usually makes the distribution of Sh on the suction surface more uniform as can be seen at *z/s* = 0.12, 0.20, and 0.50, because it suppress reattachment/ separation procedure on the suction surface as well. With increasing *z/s*, in general, the suction-side discrepancy between the two cases becomes more noticeable.

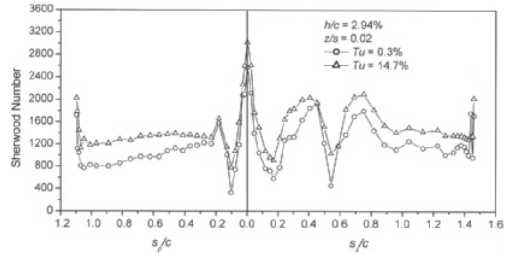

(a) *z/s* = 0.02

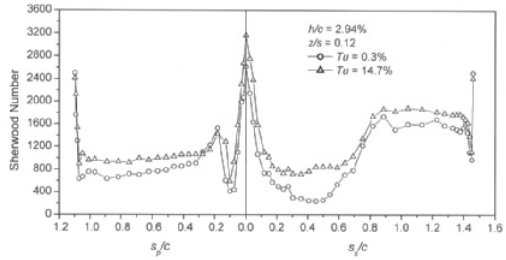

(b) *z/s* = 0.12

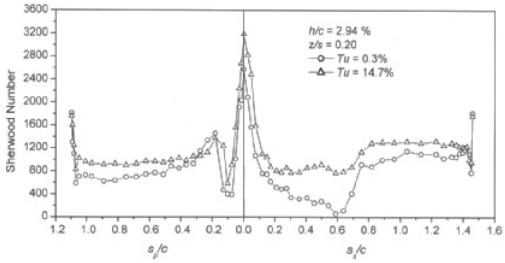

(c) *z/s* = 0.2

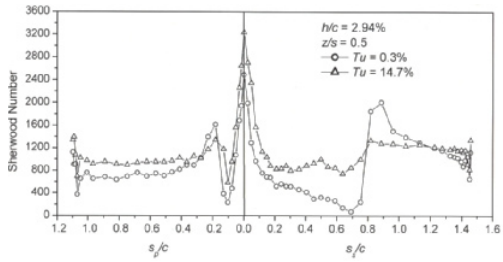

(d) *z/s* = 0.5

Fig. 7. Chord-wise profile of Sh for *h/c* = 2.94%.

Figure 8 shows the span-wise distributions of Sh at the leading and trailing edges. At the leading-edge stagnation point of s_p/c = 0.0 (Fig. 8(a)), the mid-span Sh in the high turbulence case is about 30 percent higher than that in the low turbulence case. This discrepancy tends to decrease with approaching the tip edge. The Sh profiles along the trailing-edge centerline in Fig. 8(b) are very different from those at

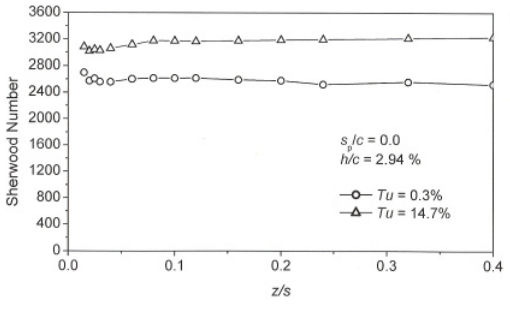

(a) s_p/c = 0.0 (leading-edge stagnation point)

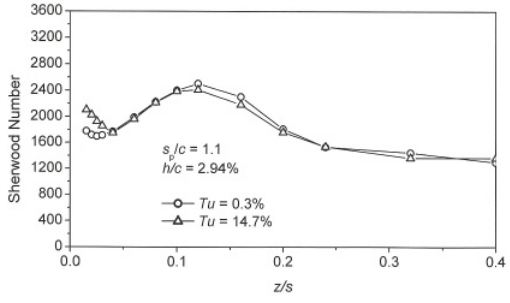

(b) s_p/c = 1.1 (trailing-edge centerline)

Fig. 8. Span-wise profile of Sh for h/c = 2.94%.

s_p/c = 0.0. As moving toward the tip edge from the mid-span, Sh increases, has a peak value at around z/s = 0.12, decreases, and then increases again, regardless of the inlet turbulence level. As mentioned earlier, the peak arises from the interaction of the tip-leakage vortex along the suction side with the trailing-edge vortex shedding. The span-wise location and the peak value are approximately the same in the two cases, which means that strength and elevation of the tip-leakage vortex remain nearly unchanged. In fact, the discrepancy between the two results is found only just near the tip edge as can be seen in Fig. 8(b).

Jin and Goldstein (2003) measured local mass transfer on a turbine blade near-tip surface. Their turbine blades had an extra high aspect ratio (span-to-chord ratio) of 2.5 and a lower turning angle of 107.5 degrees. They were mainly conducted at Tu = 0.2 percents, and provided only a limited data percents at Tu = 12 percents without any contour plots for h/c = 0.86. They concluded that this turbulence level increases the local mass transfer rates on the pressure side. This is only a high turbulence effect discussed in their study. In this study, however, a lot of discussions and conclusions are provided about the high-turbulence effects on Sh.

4. Conclusion

The near-tip blade-surface heat/mass transfer under combustor-level high inlet turbulence has been investigated within a high-turning turbine rotor passage for three tip gap-to-chord ratios of h/c = 0.74, 1.47, and 2.94 percents. The major findings are summarized as follows.

(1) There exists heat/mass transfer augmentation in the pressure-side near-tip area due to the flow acceleration near the tip edge into the tip gap. Increasing h/c results not only in higher heat/mass transfer in the pressure-side tip region but also in more convective transports over the pressure surface even far away from the tip edge.

(2) There is a local maximum of heat/mass transfer along the trailing-edge centerline, which arises from the interaction of a tip-leakage vortex with a trailing-edge vortex shedding.

(3) On the suction surface, severe heat/mass transfer is always observed in the tip-leakage flow region which is divided into two distinct areas: the upstream high transport region and the downstream one.

The present high-turbulence near-tip data for h/c = 2.94 percents is compared with the corresponding low-turbulence data. This comparison provides the following conclusions.

(4) The high inlet turbulence provides more uniform heat/mass transfer.

(5) The comparison shows that there is a large discrepancy of the pressure-side heat/mass transfer in the near-tip area particularly between the mid-chord and trailing edge, but this difference diminishes with departing from the tip edge.

(6) Heat/mass transfer in the tip-leakage flow region on the suction surface is less influenced by the high inlet turbulence than that at the mid-span, because there already exist local flow disturbances.

(7) The leading-edge heat/mass transfer in the high turbulence case is higher than that in the low turbulence case, while there is no big difference in the trailing-edge heat/mass transfer between the two cases.

Nomenclature

c	: Chord, Fig. 2
D	: Diffusion coefficient of naphthalene in air
h	: Tip clearance gap

h_m : Local mass transfer coefficient
Nu : Nusselt number
Pr : Prandtl number, ν/α
Re : Inlet Reynolds number, $U_\infty c/\nu$
s : Span, Fig. 2
s_p, s_s : curvilinear coordinates along the pressure and suction surfaces, Fig. 2
Sc : Schmidt number, ν/D
Sh : Sherwood number, $h_m c/D$
Tu : turbulence intensity
U_∞ : inlet free-stream velocity
x_D, y_D, z_D : coordinates at the inlet duct, Fig. 1
x, y, z : cascade coordinates, Fig. 2

Greek characters

α : Thermal diffusivity
ν : Kinematic viscosity

References

Abernethy, R. B., Benedict, R. P., Dowdell, R. B., 1985, "ASME Measurement Uncertainty," *ASME Journal of Fluids Engineering*, Vol. 107, pp. 161~164.

Azad, G. S., Han, J. C., Teng, S., 2000, "Heat Transfer and Pressure Distributions on a Gas Turbine Blade Tip," *ASME Journal of Turbomachinery*, Vol. 122, pp. 717~724.

Bindon, J. P., 1989, "The Measurement and Formation of Tip Clearance Loss," *ASME Journal of Turbomachinery*, Vol. 111, pp. 257~263.

Bunker, R. S., Bailey, J. C., Ameri, A. A., 2000, "Heat Transfer and Flow on the First-Stage Blade Tip of a Power Generation Gas Turbine: Part 1–Experimental Results," *ASME Journal of Turbomachinery*, Vol. 122, pp. 263~271.

Chyu, M. K., Moon, H. K., Metzger, D. E., 1989, "Heat Transfer in the Tip Region of Grooved Turbine Blades," *ASME Journal of Turbomachinery*, Vol. 111, pp. 131~138.

Goldstein, R. J., Cho, H. H., 1995, "A Review of Mass Transfer Measurements Using Naphthalene Sublimation," *Experimental Thermal and Fluid Science*, Vol. 10, pp. 416~434.

Jin, P., Goldstein, R. J., 2003, "Local Mass/Heat Transfer on Turbine Blade Near-Tip Surfaces," *ASME Journal of Turbomachinery*, Vol. 125, pp. 521~528.

Jun, S. B., 2000, Measurements of Endwall Heat (Mass) Transfer Coefficient in a Linear Turbine Cascade Using Naphthalene Sublimation Technique, MS thesis, Kumoh National Institute of Technology.

Lee, S. W., Jun, S. B., Park, B. K., Lee, J. S., 2004, "Effects of Combustor-Level Inlet Turbulence on the Endwall Flow and Heat/Mass Transfer of a High-Turning Rotor Cascade," *Journal of Mechanical Science and Technology*, Vol. 18, pp. 1435~1450.

Lee, S. W., Kwon, H. G., 2004, "Heat(Mass) Transfer Characteristics in the Tip-Leakage Flow Region of a High-Turning Turbine Rotor Cascade," *Trans. KSME (B)*, Vol. 28, pp. 535~544.

Lee, S. W., Kwon, H. G., Park, B. K., 2005, "Effects of Combustor-Level High Free-Stream Turbulence on Blade-Surface Heat/Mass Transfer in the Three-Dimensional Flow Region near the Endwall of a High-Turning Rotor Cascade," *Journal of Mechanical Sci-ence and Technology*, Vol. 19, pp. 1347~1357.

Metzger, D. E., Rued, K., 1989, "The Influence of Turbine Clearance Gap Leakage on Passage Velocity and Heat Transfer Near Blade Tips: Part I–Sink Flow Effects on Blade Pressure Sides," *ASME Journal of Turbomachinery*, Vol. 111, pp. 284~292.

Metzger, D. E., Dunn, M. G., Hah, C., 1991, "Turbine Tip and Shroud Heat Transfer," *ASME Journal of Turbomachinery*, Vol. 113, pp. 502~507.

Papa, M., Goldstein, R. J., Gori, F., 2003, "Effects of Tip Geometry and Tip Clearance on the Mass/Heat Transfer From a Large-Scale Gas Turbine Blade," *ASME Journal of Turbomachinery*, Vol. 125, pp. 90~96.

Rued, K., Metzger, D. E., 1989, "The Influence of Turbine Clearance Gap Leakage on Passage Velocity and Heat Transfer Near Blade Tips: Part II–Source Flow Effects on Blade Suction Sides," *ASME Journal of Turbomachinery*, Vol. 111, pp. 293~300.

STP 470A, 1974, *Manual on the Use of Thermocouples in Temperature Measurement*, published by ASTM.